J|A|C|S
COMMUNICATIONS

Published on Web 09/24/2004

Multiple Areas of Magnetic Bistability in the Topological Ferrimagnet $[Co_3(NC_5H_3(CO_2)_2\text{-}2,5)_2(\mu_3\text{-}OH)_2(OH_2)_2]$

Simon M. Humphrey and Paul T. Wood*

University Chemical Laboratory, University of Cambridge, Lensfield Road, Cambridge, CB2 1EW, U.K.

Received June 21, 2004; E-mail: ptw22@cam.ac.uk

Magnetic lattices containing odd-sided polyhedra with antiferromagnetic coupling have been the focus of intense study because the spin frustration inherent in these materials induces unusual types of magnetic behavior such as spin liquid[1,2] and spin ice[3,4] phases. These materials are invariably based on triangular plaquettes, and for ideal spin frustration the triangles must be equilateral. However, similar materials containing scalene triangles are also of interest because the competing interactions can give rise to various types of magnetic order. In combination with metal ions possessing different g values, this may produce complex magnetic phase behavior of interest to theoreticians. In addition, materials displaying magnetic bistability (hysteresis) are of great interest because of the search for new and more efficient magnetic recording materials.

Here we report the solvothermal synthesis of a new Co(II) coordination solid $[Co_3(NC_5H_3(CO_2)_2\text{-}2,5)_2(\mu_3\text{-}OH)_2(OH_2)_2]$ (**1**) whose structure was determined by X-ray diffraction analysis. Reaction of cobalt(II) chloride with pyridine-2,5-dicarboxylic acid and KOH in a molar ratio of 3:2:7 in water at 230 °C afforded deep purple needles of **1** in 54% yield.

The asymmetric unit of **1** (Figure 1)[5,6] contains three distinct Co(II) environments. Co1 is a distorted trigonal bipyramid, while the coordination geometry of Co2 is intermediate between trigonal bipyramidal and square-based pyramidal; both have M-NCCO chelate rings with similar bite angles (77.9(3) and 76.4(3)°, respectively). Co3 is pseudo-octahedrally coordinated to an oxygen-only donor set, comprised of trans coordination by carboxylate-*O* and equatorial cis coordination of OH_2 and μ_3-hydroxide (O5 and O6) ligands. Co1 and Co2 are connected via O5 and O6 μ_3-hydroxide moieties, resulting in a chain of hydroxide-bridged scalene triangles that share edges and vertexes (Figure 2): Co1 and Co3 form the shared edge, while Co2 is at the shared vertex. Co3 is bridged in *syn-syn* fashion to Co1 by an O3−C8−O4 carboxylate moiety approximately orthogonal to the plane of the hydroxide-bridged chain. Co3 is also linked to Co2 equivalents in an adjacent chain via a further carboxylate bridge. These interactions lead to pairs of adjacent chains being *syn-anti*-carboxylate bridged via $(Co2-O11-C17-O12-Co3)_2$ units. Parallel chains of Co(II) triangles are out-of-phase along the crystallographic a-axis by $a/2$.

When viewed in the *ac*-plane, the extended structure of **1** is a close-packed grid of ladders where adjacent pairs of Co(II) chains are separated by aromatic moieties (Figure 3a). When viewed in the *bc*-plane, the lattice is much less dense since small diamond-shaped voids are present (Figure 3b). Coordinated OH_2 molecules project into these areas, and hydroxide-*H* atoms point into the center of the 10-membered cobalt−carboxylate rings. The VOID utility in the program PLATON[7] suggests that there is no significant solvent-accessible space within **1**.

The DC susceptibility of a polycrystalline sample of **1** was measured on a Quantum Design MPMS-5 SQUID magnetometer. The material obeys Curie−Weiss law down to 125 K with $C = 8.60(6)$ cm^3 mol^{-1} K^{-1} and $\Theta = -56(2)$ K. This is consistent with

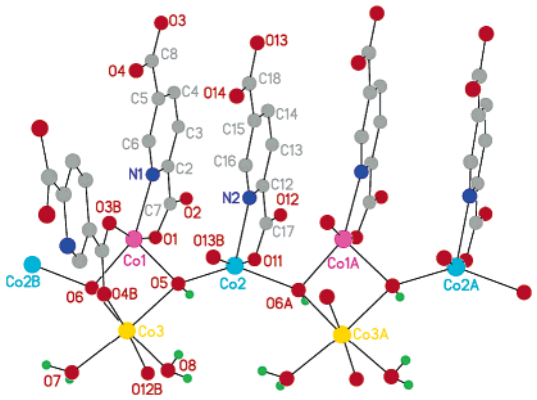

Figure 1. Crystal structure of **1** showing complete coordination environments of the three cobalt(II) environments. Aromatic hydrogen atoms are omitted for clarity (all other hydrogen atoms drawn in green).

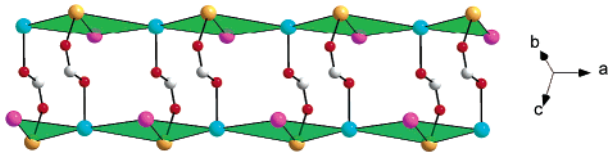

Figure 2. Parallel chains of edge- and vertex-sharing triangles in **1** with *syn-anti*-carboxylate bridges. Green triangles have μ_3-hydroxide-*O* at their center (omitted).

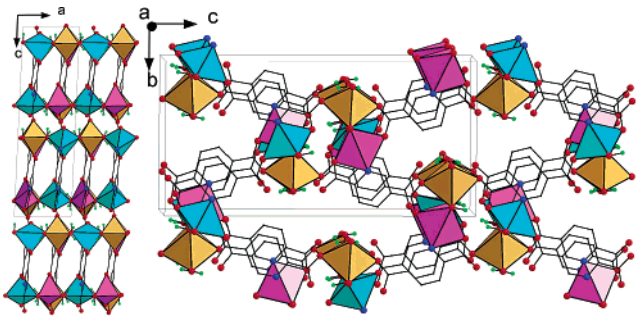

Figure 3. a (left) and b (right): Projections of crystal packing arrangements in **1**. Co(II) polyhedra and other atoms are shown in colors corresponding to those in Figure 1.

three $S = 3/2$ ions with moderate antiferromagnetic coupling yielding an average g value of 2.47. It is important to remember that the single-ion anisotropy of the metal ions will also contribute to the Weiss constant, and it is not purely a measure of the magnetic exchange interaction. In small fields below 30 K (Figure 4), the susceptibility *increases* as the measuring field *decreases*, which is consistent with canted antiferromagnetism[8] producing a small but significant coercive field of 200 G (Figure 5 insert). The source of the antisymmetric exchange interaction necessary for this is the significant spin−orbit coupling associated with the $^4T_{1g}$ ground term of Co(II). A suggestion for the spin arrangement in this phase is

10.1021/ja046351l CCC: $27.50

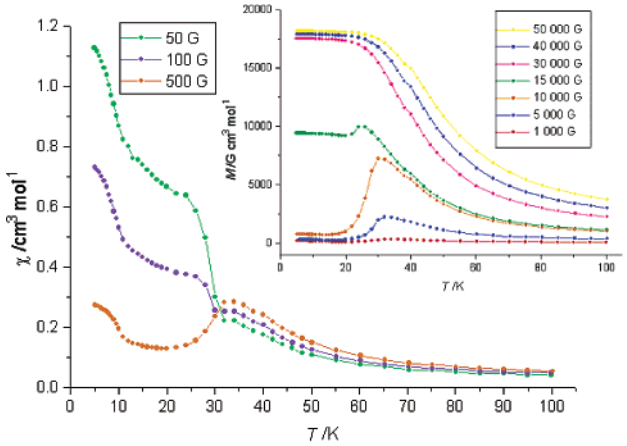

Figure 4. Plot of Chi versus *T* for **1** in small external applied fields, with magnetization data in larger applied external fields (inset).

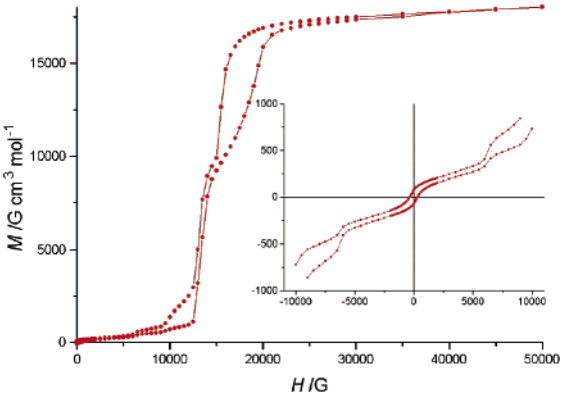

Figure 5. Hysteresis loop for partially aligned **1** recorded at 5.0 K, zero-field region inset.

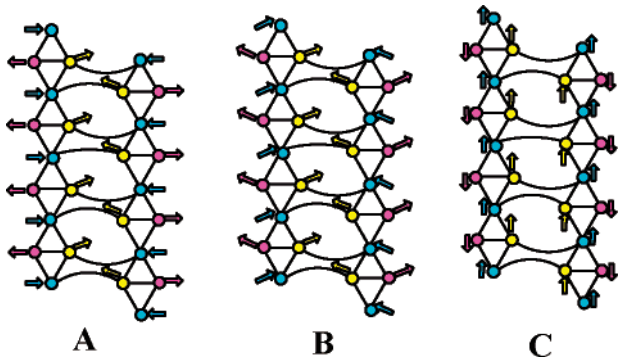

Figure 6. Suggested arrangement for the spins on the cobalt ions for (a) $H < 10\,000$ G, (b) $10\,000 < H < 15\,000$ G, and (c) $H > 15\,000$ G. The chains are as shown in Figure 2.

shown in Figure 6A. Between 5000 and 12 000 G, a spin flip phase (the nature of which is suggested in Figure 6B) is responsible for a second area of bistability. At fields in excess of 15 000 G, a third area of bistability may be observed due to a field-induced reorientation of the spins. The magnetization saturates at slightly more than 18 000 G cm^3 mol^{-1} compared with 62 077 G cm^3 mol^{-1} calculated for ferromagnetic alignment, which suggest a spin structure in which 1/3 of the Co(II) ions are uncompensated (e.g., as shown in Figure 6C).

We have compared the *M* vs *H* plots for polycrystalline **1** immobilized in a frozen Nujol matrix with a sample compressed in a gelatin capsule.[9] This shows that field-induced alignment of the sample occurs in small fields so that the plot shown in Figure 5 is that of a sample with its easy axis predominantly parallel to the applied field. The measurement was then repeated with the partially aligned sample immobilized in Nujol: this produced a plot very similar in form to Figure 5, demonstrating that the discontinuities are not caused by sudden reorientations of the sample crystallites. Finally, the sample was randomized within the Nujol matrix and the measurement repeated. In this case, all the areas of bistability remain but are much less pronounced, as would be expected when a smaller proportion of the sample has its easy axis parallel to the applied field.

Magnetic bistability may be observed in materials with ferromagnetic, ferrimagnetic, canted antiferromagnetic, or metamagnetic spin arrangements, but it is very rare to observe more than one area of bistability for a single material. We ascribe the behavior of **1** to the competing superexchange and dipolar exchange pathways, the different *g* values associated with different coordination geometries, and the structural anisotropy of the material.

Acknowledgment. We thank Prof. Mary McPartlin (University of North London) and Dr. John E. Davies (University of Cambridge) for their advice regarding the crystal structure and Prof. Fernando Palacio (Zaragoza, Spain) for helpful discussions on the magnetic data. We thank the EPSRC for funding and for contributing to the purchase of the CCD diffractometer.

Supporting Information Available: Crystallographic data (CIF) and full experimental preparation with characterizing data for **1** (PDF). This material is available free of charge via the Internet at http://pubs.acs.org.

References

(1) Lee, S. H.; Broholm, C.; Ratcliff, C.; Gasparovic, G.; Huang, Q.; Kim. T. H.; Cheong, S. W. *Nature* **2002**, *418*, 856.
(2) Fritsch, V.; Hemberger, J.; Buttgen, N.; Scheidt, E. W.; von Nidda, H. A. K,; Loidl, A.; Tsurkan, V. *Phys. Rev. Lett.* **2004**, *92*, 116401
(3) Bramwell, S. T.; Gingras, M. J. P *Science* **2001**, *294*, 1495.
(4) Snyder, J.; Slusky, J. S.; Cava, R. J.; Schiffer, P. *Nature* **2001**, *413*, 48.
(5) Crystal data for **1**: $[Co_3(NC_5H_3(CO_2)_2\text{-}2,5)_2(\mu_3\text{-}OH)_2(OH_2)_2]$, $C_{14}H_{12}Co_3N_2O_{12}$, $M = 577.05$, monoclinic, space group $P2_1/n$, $a = 6.6426(2)$ Å, $b = 11.3188(4)$ Å, $c = 22.6559(10)$ Å, $\beta = 92.6329(15)°$, $V = 1701.63(11)$ Å^3, $Z = 4$, $T = 180(2)$ K. Refinement of 292 paramaters on 2859 independent reflections out of 9111 total measured reflections ($R_{int} = 0.0644$) led to $R_1 = 0.072$, w$R_2 = 0.158$, and $S = 1.077$.
(6) Sheldrick, G. M. *SHELXTL*, Version 6.10; Bruker AXS, Inc.: Madison, WI, 2001.
(7) *PLATON*, Version 1.07: Spek, A. L. *J. Appl. Crystallogr.* **2003**, *36*, 7.
(8) Kahn, O. *Molecular Magnetism*; Wiley-VCH: New York, 1993.
(9) We would like to thank a referee for this suggestion.

JA046351L